Cell-level anatomical characteristics explain high mesophyll conductance and photosynthetic capacity in sclerophyllous Mediterranean oaks

José Javier Peguero-Pina[1,2]*, Sergio Sisó[1]*, Jaume Flexas[3], Jeroni Galmés[3], Ana García-Nogales[4], Ülo Niinemets[5], Domingo Sancho-Knapik[1,2], Miguel Ángel Saz[6] and Eustaquio Gil-Pelegrín[1,2]

[1]Unidad de Recursos Forestales, Centro de Investigación y Tecnología Agroalimentaria de Aragón, Gobierno de Aragón, Avda. Montañana 930, 50059 Zaragoza, Spain; [2]Instituto Agroalimentario de Aragón -IA2- (CITA-Universidad de Zaragoza), 50013 Zaragoza, Spain; [3]Research Group on Plant Biology under Mediterranean Conditions, Departament de Biologia, Universitat de les Illes Balears, Carretera de Valldemossa km 7.5, 07122 Palma de Mallorca, Spain; [4]Department of Physical, Chemical and Natural Systems, University Pablo Olavide, Carretera de Utrera km 1, 41013 Sevilla, Spain; [5]Institute of Agricultural and Environmental Sciences, Estonian University of Life Sciences, Kreutzwaldi 1, Tartu 51014, Estonia; [6]Departamento de Geografía y Ordenación del Territorio, Universidad de Zaragoza, 50009 Zaragoza, Spain

Author for correspondence:
Eustaquio Gil-Pelegrín
Tel: +34 976 716394
Email: egilp@aragon.es

Summary

- Leaf mass per area (LMA) has been suggested to negatively affect the mesophyll conductance to CO_2 (g_m), which is the most limiting factor for area-based photosynthesis (A_N) in many Mediterranean sclerophyll species. However, despite their high LMA, these species have similar A_N to plants from other biomes. Variations in other leaf anatomical traits, such as mesophyll and chloroplast surface area exposed to intercellular air space (S_m/S and S_c/S), may offset the restrictions imposed by high LMA in g_m and A_N in these species.
- Seven sclerophyllous Mediterranean oaks from Europe/North Africa and North America with contrasting LMA were compared in terms of morphological, anatomical and photosynthetic traits.
- Mediterranean oaks showed specific differences in A_N that go beyond the common morphological leaf traits reported for these species (reduced leaf area and thick leaves). These variations resulted mainly from the differences in g_m, the most limiting factor for carbon assimilation in these species.
- Species with higher A_N showed increased S_c/S, which implies increased g_m without changes in stomatal conductance. The occurrence of this anatomical adaptation at the cell level allowed evergreen oaks to reach A_N values comparable to congeneric deciduous species despite their higher LMA.

Introduction

Mediterranean-type ecosystems are characterized by the presence of woody evergreen sclerophyllous species that exhibit high leaf dry mass per unit area (LMA) (Kummerow, 1973; Galmés *et al.*, 2005, 2012), with small and thickened leaves (Traiser *et al.*, 2005). This vegetation type includes several species of the genus *Quercus* (Fagaceae), the so-called Mediterranean oaks, that can be found in Mediterranean-type evergreen woodlands of Europe and North America (Manos *et al.*, 1999; Kremer *et al.*, 2012). These species belong to different infrageneric groups (Denk & Grimm, 2009), but share common convergent leaf morphological and functional traits including high LMA (Corcuera *et al.*, 2002).

LMA is considered a key structural trait that has the potential to negatively affect the mass-based photosynthetic performance of the plant (Wright *et al.*, 2004, 2005), which has been associated with a higher investment in nonphotosynthetic tissue and/or a lower efficiency of the photosynthetically active mesophyll (Niinemets *et al.*, 2009; Hassiotou *et al.*, 2010). When considered globally, the relationship between LMA and area-based net CO_2 assimilation (A_N) is less clear. However, an essential component of A_N, the mesophyll conductance to CO_2 (g_m), has been shown to be negatively related to LMA (Flexas *et al.*, 2008). Hence, as g_m is the most limiting factor for A_N in many Mediterranean sclerophyll species (Roupsard *et al.*, 1996; Piel, 2002; Flexas *et al.*, 2014; Galmés *et al.*, 2014; Niinemets & Keenan, 2014; Peguero-Pina *et al.*, 2016a), a negative relationship between A_N and LMA is expected, at least within this group of species. Accordingly, Hassiotou *et al.* (2009) found that A_N tended to be lower as LMA increased for seven species of the Australian sclerophyllous genus *Banksia* covering a wide range of high LMA. These authors also found that high-LMA species

*These authors contributed equally to this work.

showed a significantly lower CO_2 diffusion conductance from substomatal cavities to the chloroplasts (i.e. g_m).

The fact that g_m is constrained by large LMA (which can be explained by increases in leaf thickness and/or leaf density) has been mostly related to: (1) an increase in the resistance of the CO_2 gas-phase conductance associated with greater leaf thickness and density (Niinemets *et al.*, 2009; Hassiotou *et al.*, 2010; Tosens *et al.*, 2012a; Tomás *et al.*, 2013), and (2) the thicker cell walls observed in species with high leaf density, significantly limiting CO_2 diffusion in the leaf liquid phase (Peguero-Pina *et al.*, 2012; Tosens *et al.*, 2012a; Tomás *et al.*, 2013). Therefore, Mediterranean plants with high LMA – including Mediterranean oaks – would be expected to present lower photosynthetic capacities than species from other biomes with lower LMA. However, contrary to expectations, Flexas *et al.* (2014) found that despite having higher average LMA, Mediterranean species, on average, have similar photosynthetic capacity on an area basis as plants from any other biomes. In fact, Peguero-Pina *et al.* (2009) reported values of net CO_2 assimilation rate for Mediterranean oaks *Quercus coccifera*, *Quercus ilex* and *Quercus suber* that were very similar to those found in other temperate oak species with lower LMA, such as *Quercus robur*, *Quercus petraea*, *Quercus cerris*, *Quercus rubra* or *Quercus prinus* (Epron *et al.*, 1992, 1993; Valentini *et al.*, 1995; Turnbull *et al.*, 2002; Cano *et al.*, 2013; Steinbrecher *et al.*, 2013; Peguero-Pina *et al.*, 2016b). A possible explanation for these contradictory findings was provided by Flexas *et al.* (2014), who hypothesized that high LMA in Mediterranean species is also responsible for the enhanced capacity of carboxylation per area ($V_{c,max}$) due to increased Rubisco content per area in thicker leaves with more cell layers.

Variation in LMA in Mediterranean oaks is primarily driven by variations in leaf thickness and to a lesser degree in the other component of LMA, leaf density (Niinemets, 2015; González-Zurdo *et al.*, 2016). Besides LMA and leaf thickness, there are other leaf structural and anatomical traits, including packing of mesophyll cells relative to each other, thickness of mesophyll cell walls, leaf airspace volume (the aforementioned traits are the primary determinants of leaf density), packing of mesophyll cells relative to the distance and position of stomata, mesophyll and chloroplast surface area exposed to intercellular air space per unit of leaf area (S_m/S and S_c/S, respectively) and chloroplast size, that quantitatively determine the variability in g_m and photosynthetic capacity among species (Tomás *et al.*, 2013; Peguero-Pina *et al.*, 2016b) or even within the same species growing under contrasting environmental conditions (Terashima *et al.*, 2011; Tosens *et al.*, 2012b; Peguero-Pina *et al.*, 2016a,c). Variations in such cellular or whole leaf traits could positively influence g_m and, consequently, net CO_2 assimilation in evergreen sclerophyllous species with large LMA values. Several studies have indicated that leaves with thicker mesophyll have larger S_m/S and/or S_c/S, implying a greater g_m in thicker leaves (Hanba *et al.*, 1999, 2002; Terashima *et al.*, 2006; Peguero-Pina *et al.*, 2016b). This could be interpreted as a way for improving photosynthesis in species with high LMA. However, other studies call into question the generality of such a mechanism, because they did not find a correlation between leaf thickness and S_m/S (Slaton & Smith, 2002) or S_c/S (Tosens *et al.*, 2012a).

The Mediterranean oaks constitute an excellent framework to elucidate the existence of anatomical and/or biochemical adaptations that may offset the restrictions imposed by high LMA in g_m and A_N. Furthermore, regardless of the convergence in overall leaf appearance, Corcuera *et al.* (2002) pointed out that Mediterranean oaks showed a high dispersion in their LMA values despite their 'sclerophyllous condition', contrary to the patterns in deciduous temperate and warm temperate Mediterranean oak species. Therefore, we hypothesize that: (1) these differences in LMA among the Mediterranean oaks would also be expressed in terms of specific differences in photosynthetic activity on an area basis (A_N); and (2) the presence of anatomical adaptations (e.g. increased S_m/S or S_c/S) would allow these evergreen oaks to reach A_N values comparable to congeneric deciduous species despite their higher LMA (Corcuera *et al.*, 2002) and lower stomatal conductance (Peguero-Pina *et al.*, 2009), two factors that could limit the photosynthetic activity in the Mediterranean oaks. To test these hypotheses, in this study we compared the morphological, anatomical and photosynthetic traits and the share of different photosynthetic limitations of seven Mediterranean oaks from Europe/North Africa and North America in a common garden.

Materials and Methods

Plant material and experimental conditions

Seven representative evergreen sclerophyllous Mediterranean oak species from Europe/North Africa and North America belonging to different infrageneric groups (Denk & Grimm, 2009) were studied: *Ilex* group (*Q. coccifera* L., *Q. ilex* subsp. *rotundifolia* Lam. and *Q. ilex* subsp. *ilex* L.), *Cerris* group (*Q. suber* L.), *Lobatae* group (*Quercus agrifolia* Née. and *Quercus wislizeni* A. DC.) and *Protobalanus* group (*Quercus chrysolepis* Liebm.) (Table 1). The seeds of the seven species were collected from one population per species (see Table 1 for details), sown in 2009 and cultivated in 0.5 l containers inside a glasshouse under the same conditions with a mixture of 80% compost (Neuhaus Humin Substrat N6; Klasman-Deilmann GmbH, Geeste, Germany) and 20% perlite. After the first growth cycle, the seedlings were transplanted to 25 l containers filled with the same mixture of compost and perlite and cultivated outdoors at CITA de Aragón (41°39′N, 0°52′W, Zaragoza, Spain) under Mediterranean conditions (mean annual temperature 15.4°C, total annual precipitation 298 mm). Nutrients were supplied as slow-release fertilizer (Osmocote Plus, Sierra Chemical, Milpitas, CA, USA). The fertilizer (3 g l^{-1} growth substrate) was applied to the top 10 cm layer of substrate. All plants were grown under the same environmental conditions and drip-irrigated every 2 d. Each potted plant was located in the centre of a plastic pallet of 1 m^2, which ensured a minimum distance among plants. We used 10 4-yr-old plants per species of similar size (*c.* 65 cm height and 20 mm in basal diameter), so the area of the experimental field was 70 m^2. The position of each plant was randomized within the experimental field. The measurements were carried out in summer 2012 using

Table 1 Geographical origin, infrageneric classification, exact location and mean climatic characteristics where seeds were collected for the seven studied *Quercus* species

Species	Origin	Group	Latitude	Longitude	T (°C)	T_s (°C)	P (mm)	P_s (mm)	MAI	Gaussen index
Q. chrysolepis	North America	Protobalanus	39°27′N	123°05′W	12.5	19.4	1114	14	49	5
Q. agrifolia	North America	Lobatae	39°18′N	123°45′W	14.3	19.1	954	15	39	5
Q. wislizeni	North America	Lobatae	34°16′N	118°04′W	15.4	23.4	851	13	34	5
Q. coccifera	Europe/North Africa	Ilex	41°47′N	00°30′W	12.4	20.8	440	79	20	3
Q. ilex subsp. ilex	Europe	Ilex	41°13′N	13°03′E	15.5	22.4	940	83	34	3
Q. ilex subsp. rotundifolia	Europe/North Africa	Ilex	41°46′N	02°29′W	10.9	19.2	514	104	25	2
Q. suber	Europe/North Africa	Cerris	40°10′N	06°14′W	15.0	23.8	469	37	19	4

T and T_s, mean annual and summer temperature; P and P_s, total annual and summer precipitation; MAI, Martonne's aridity index.

current-year fully developed leaves and just before irrigation (at field capacity), when predawn water potential was below −0.1 MPa (data not shown).

Although the distribution ranges of the studied species (Supporting Information Fig. S1) are typically Mediterranean with summer drought, there are slight differences among species in the climate at origins (Table 1; Figs S2, S3). Climatic information was obtained for the studied species from the WorldClim database (http://www.worldclim.org/) using geographical points throughout the distribution range of each species (Fig. S1). To quantify aridity, we calculated Martonne's aridity index (MAI = P/(T + 10)) and Gaussen index (the number of months in which P < 2T, where P is monthly precipitation in mm and T is monthly mean temperature in °C). Moreover, the maximum daily vapour pressure deficit (VPD$_{max}$, kPa) (Fig. S3) was calculated using data obtained from the WeatherSpark database (http://weatherspark.com/).

Leaf gas exchange and chlorophyll fluorescence measurements

Leaf gas exchange and chlorophyll fluorescence parameters were measured simultaneously using an open gas exchange system (CIRAS-2; PP-Systems, Amesbury, MA, USA) fitted with an automatic universal leaf cuvette (PLC6-U; PP-Systems) and an FMS II portable pulse amplitude modulated fluorometer (Hansatech Instruments Ltd, King's Lynn, UK). Six CO_2 response curves were measured per species using light-adapted mature leaves. The photosynthesis measurements started at a CO_2 concentration surrounding the leaf (C_a) of 400 µmol mol^{-1}, and a saturating photosynthetic photon flux density (PPFD) of 1500 µmol m^{-2} s^{-1}. Leaf temperature and VPD were maintained at 25°C and 1.25 kPa, respectively, during all measurements. Once the steady state gas exchange rate was reached under these conditions (usually in 30 min after clamping the leaf), net assimilation rate (A_N), stomatal conductance (g_s) and the effective quantum yield of photosystem II (PSII; Φ_{PSII}) were estimated. Thereafter, C_a was decreased stepwise down to 50 µmol mol^{-1}. Upon completion of the measurements at low C_a, C_a was increased again to 400 µmol mol^{-1} to restore the original value of A_N. C_a was further increased stepwise to 1800 µmol mol^{-1}

and all the steady-state photosynthetic characteristics were recorded at each C_a. Leakage of CO_2 in and out of the cuvette was determined for the same range of CO_2 concentrations with a photosynthetically inactive leaf enclosed (obtained by heating the leaf until no variable chlorophyll fluorescence was observed), and used to correct for measured leaf fluxes (Flexas *et al.*, 2007a).

For Φ_{PSII}, the steady-state fluorescence (F_S) and the maximum fluorescence during a light-saturating pulse of *c.* 8000 µmol m^{-2} s^{-1} (F'_M) were estimated, and Φ_{PSII} was calculated as (F'_M − F_S)/F'_M (Genty *et al.*, 1989). Photosynthetic electron transport rate (J_F) was then calculated according to Krall & Edwards (1992), multiplying Φ_{PSII} by PPFD and by α (a term which includes the product of leaf absorptance and the partitioning of absorbed quanta between PSI and II). The term α was previously determined as the slope of the relationship between Φ_{PSII} and Φ_{CO2} (i.e. the quantum efficiency of CO_2 fixation) obtained by varying light intensity under nonphotorespiratory conditions in an atmosphere containing <1% O_2 (Valentini *et al.*, 1995). Five photosynthesis vs PPFD response curves were measured per species to determine α.

Estimation of mesophyll conductance, g_m, by gas exchange and chlorophyll fluorescence

Mesophyll conductance (g_m) was estimated according to the method of Harley *et al.* (1992), as follows:

$$g_m = \frac{A_N}{C_i - \frac{\Gamma^*(J_F + 8(A_N + R_L))}{J_F - 4(A_N + R_L)}} \qquad \text{Eqn 1}$$

where A_N and the substomatal CO_2 concentration (C_i) were taken from the gas exchange measurements at saturating light, whereas Γ^* (the chloroplastic CO_2 compensation point in the absence of mitochondrial respiration) and R_L (the respiration rate in the light) were estimated for each species following the method described by Flexas *et al.* (2007b). The values of g_m obtained were used to convert A_N−C_i responses into A_N−C_c responses (where C_c is the chloroplastic CO_2 concentration) using the equation $C_c = C_i − A_N/g_m$. The maximum ribulose-1,5-bisphosphate carboxylation ($V_{c,max}$) and photosynthetic electron transport (J_{max}) capacities were calculated from the A_N−C_c curves, using

the Rubisco kinetic constants and their temperature dependencies described by Bernacchi *et al.* (2002). The model of Farquhar *et al.* (1980) was fitted to the data by applying iterative curve-fitting (minimum least-square difference) using the Solver tool of Microsoft Excel.

Morphological and anatomical measurements

After the gas exchange measurements, sections of 1×1 mm were cut between the main veins for anatomical measurements from the same leaves used for gas exchange (one leaf per plant from six plants per species). Leaf material was quickly fixed under vacuum with 2% *p*-formaldehyde (2%) and glutaraldehyde (4%) in 0.1 M phosphate buffer solution (pH 7.2) and post-fixed for 1 h in 1% osmium tetroxide. Samples were dehydrated in: (1) a graded ethanol series and (2) propylene oxide and subsequently embedded in Embed-812 embedding medium (EMS, Hatfield, PA, USA). Semi-thin (0.8 μm) and ultrathin (90 nm) cross-sections were cut with an ultramicrotome (Reichert & Jung model Ultracut E). Semi-thin cross-sections were stained with 1% toluidine blue and viewed under a light microscope (Optika B-600TiFL, Optika Microscopes, Ponteranica, Italy). Ultrathin cross-sections were contrasted with uranyl acetate and lead citrate and viewed under a transmission electron microscope (H600, Hitachi, Tokyo, Japan). IMAGEJ software (http://rsb.info.nih.gov/nih-image/) was further used to measure leaf anatomical characteristics from the micrographs. Light microscopy images were used to determine leaf thickness, mesophyll thickness between the two epidermal layers, number of palisade layers and the fraction of the mesophyll tissue occupied by the intercellular air spaces (f_{ias}) (Syvertsen *et al.*, 1995; Tomás *et al.*, 2013). S_m/S and S_c/S were calculated from light and electron micrographs following the method of Syvertsen *et al.* (1995). Thus, S_m/S is given as:

$$S_{mes}/S = \frac{L_{mes}}{W} \gamma \qquad \text{Eqn 2}$$

where W is the width of the section measured, and L_{mes} is the total length of mesophyll cells facing the intercellular airspace. The curvature correction factor (γ), which depends on the shape of the cells (Evans *et al.*, 1994), was measured and calculated for each species according to Thain (1983) for palisade and spongy cells by measuring their width and height and calculating an average width/height ratio. Analogously, S_c/S was calculated as:

$$S_c/S = \frac{L_c}{L_{mes}} S_{mes}/S \qquad \text{Eqn 3}$$

where L_c is the total length of chloroplast surface area facing the intercellular airspace in the section. Electron micrographs were used to determine cell wall thickness (T_{cw}), cytoplasm thickness (T_{cyt}), chloroplast length (i.e. the major axis length of the chloroplast parallel to the cell wall, L_{chl}) and chloroplast thickness (i.e. the minor axis length of the chloroplast perpendicular to the cell wall, T_{chl}) (Tomás *et al.*, 2013). Three different sections and four to six different fields of view per leaf were used for measurements of each anatomical characteristic.

LMA was measured in 30 mature leaves sampled from 10 individuals per species (i.e. three leaves were randomly taken and the average LMA was calculated from each individual). Leaf area was measured after scanning the leaves with the IMAGEJ software. Leaves were then oven dried at 70°C for 3 d to determine their dry mass. LMA was calculated as the ratio of foliage dry mass to foliage area.

Mesophyll conductance modelled on the basis of anatomical characteristics

Leaf anatomical characteristics were used to estimate mesophyll conductance (g_m) as a composite conductance for within-leaf gas and liquid diffusion pathways, according to the one-dimensional gas diffusion model of Niinemets & Reichstein (2003) as applied by Tosens *et al.* (2012b):

$$g_m = \frac{1}{\frac{1}{g_{ias}} + \frac{R \cdot T_k}{H \cdot g_{liq}}} \qquad \text{Eqn 4}$$

where g_{ias} is the gas phase conductance inside the leaf from sub-stomatal cavities to the outer surface of cell walls, g_{liq} is the conductance in the leaf liquid and lipid phases from the outer surface of cell walls to chloroplasts, R is the gas constant (Pa m^3 K^{-1} mol^{-1}), T_k is absolute temperature (K) and H is Henry's law constant for CO_2 (Pa m^3 mol^{-1}). g_m is defined as a gas-phase conductance, and thus $H/(RT_k)$, the dimensionless form of Henry's law constant, is needed to convert g_{liq} to corresponding gas-phase equivalent conductance (Niinemets & Reichstein, 2003).

The intercellular gas-phase conductance (and the reciprocal term, r_{ias}) was obtained according to Niinemets & Reichstein (2003) as:

$$g_{ias} = \frac{1}{r_{ias}} = \frac{D_A \cdot f_{ias}}{\Delta L_{ias} \cdot \tau} \qquad \text{Eqn 5}$$

where ΔL_{ias} (m) is the average gas-phase thickness, τ is the diffusion path tortuosity (1.57 m m^{-1}, Syvertsen *et al.*, 1995), D_A is the diffusivity of CO_2 in air (1.51×10^{-5} m^2 s^{-1} at 25°C) and f_{ias} is the fraction of intercellular air spaces. ΔL_{ias} was taken as half the mesophyll thickness. Total liquid phase conductance (g_{liq}) from the outer surface of cell walls to the carboxylation sites in the chloroplasts is the sum of serial resistances of the cell wall (r_{cw}), the plasmalemma (r_{pl}) and inside the cell ($r_{cel,tot}$) (Tomás *et al.*, 2013):

$$g_{liq} = \frac{S_m}{(r_{cw} + r_{pl} + r_{cel,tot}) \cdot S} \qquad \text{Eqn 6}$$

The conductance of the cell wall was calculated as previously described by Peguero-Pina *et al.* (2012). For conductance of the plasma membrane we used an estimate of 0.0035 m s^{-1} as previously suggested (Tosens *et al.*, 2012b). The conductance inside the cell was calculated following the methodology described by Tomás *et al.* (2013), considering two different pathways of CO_2 inside the cell: one for cell wall parts lined with chloroplasts and the other for interchloroplastial areas (Tholen *et al.*, 2012).

Analysis of quantitative limitations of A_N

To separate the relative controls on A_N resulting from limited stomatal conductance (l_s), mesophyll diffusion (l_m) and biochemical capacity (l_b), we used the quantitative limitation analysis of Grassi & Magnani (2005) as applied by Tomás *et al.* (2013). Different fractional limitations, l_s, l_m and l_b ($l_s + l_m + l_b = 1$), were calculated as:

$$l_s = \frac{g_{tot}/g_s \cdot \partial A_N/\partial C_c}{g_{tot} + \partial A_N/\partial C_c} \qquad \text{Eqn 7}$$

$$l_m = \frac{g_{tot}/g_m \cdot \partial A_N/\partial C_c}{g_{tot} + \partial A_N/\partial C_c} \qquad \text{Eqn 8}$$

$$l_b = \frac{g_{tot}}{g_{tot} + \partial A_N/\partial C_c} \qquad \text{Eqn 9}$$

where g_s is the stomatal conductance to CO_2, g_m is the mesophyll conductance according to Harley *et al.* (1992; Eqn 1) and g_{tot} is the total conductance to CO_2 from ambient air to chloroplasts (sum of the inverse CO_2 serial conductances g_s and g_m). $\partial A_N/\partial C_c$ was calculated as the slope of $A_N - C_c$ response curves over a C_c range of 50–100 µmol mol^{-1}. Quantitative limitations of photosynthesis were estimated for at least five different leaves for each species, and average estimates of the component photosynthetic limitations were calculated.

Quantitative analysis of partial limitations of g_m

The determinants of g_m were divided between the component parts of the diffusion pathway (Eqns 4–6) as in Tomás *et al.* (2013). The proportion of g_m determined by limited gas-phase conductance (l_{ias}) was calculated as:

$$l_{ias} = \frac{g_m}{g_{ias}} \qquad \text{Eqn 10}$$

The share of g_m by different components of the cellular phase conductances (l_i) was determined as:

$$l_i = \frac{g_m}{g_i \frac{S_m}{S}} \qquad \text{Eqn 11}$$

where l_i is the component limitation in the cell walls, the plasmalemma and inside the cells, and g_i refers to the component diffusion conductances of the corresponding diffusion pathways.

Statistical analyses

Data are expressed as means ± standard error. One-way ANOVAs were performed to identify the species effect on photosynthetic, morphological and anatomical traits (see ANOVA outputs in Table S1). Traits among species were compared by posthoc Tukey's Honest Significant Difference test. Regarding LMA and leaf area, ANOVAs were performed using the mean values per plant as individual values. Regarding the remaining morphological and anatomical traits, ANOVAs was performed using the mean values per leaf as individual values. The effect of S_c/S_m on the linear relationship between A_N (the dependent variable) and S_m/S (the independent variable) was analysed by analysis of the variance–covariance using the GLM procedure (Dunn & Clark, 1987). The terms included in the model were: S_c/S_m (allowing for different intercepts for each group of species), S_m/S (included as a covariate) and their interaction (allowing for different slopes for each group of species), which were considered as fixed effects. If the interaction between S_c/S_m and S_m/S is not significant, a common slope can be assumed. All statistical analyses were carried out using SAS version 8.0 (SAS, Cary, NC, USA).

Results

Variation in photosynthetic capacities and mesophyll conductance among Mediterranean evergreen oaks

The correlation between LMA and A_N for the seven studied *Quercus* species was not statistically significant at $P < 0.05$ ($r^2 = 0.43$, $P = 0.10$; Fig. 1). The values of A_N and g_m showed statistically significant differences ($P < 0.05$) between the studied species, ranging from 7.6 ± 0.2 µmol CO_2 m^{-2} s^{-1} and 0.029 ± 0.002 mol CO_2 m^{-2} s^{-1} for *Q. agrifolia* to 15.6 ± 0.5 µmol CO_2 m^{-2} s^{-1} and 0.093 ± 0.006 mol CO_2 m^{-2} s^{-1} for *Q. suber* (Table 2). By contrast, no differences at $P < 0.05$ were detected in g_s and intrinsic water use efficiency (iWUE $= A_N/g_s$) among the studied species (Table 2). Parameters of the Farquhar *et al.* (1980) model of photosynthesis, $V_{c,max}$ and J_{max}, were not statistically different among species ($P > 0.05$), except for *Q. ilex* subsp. *rotundifolia* (Table 2). Thus, species differences in A_N were primarily driven by g_m and the correlation between g_m and A_N ($r^2 = 0.87$, $F = 258.8$, $P < 0.0001$; Fig. 2b) was stronger than that found between g_s and A_N ($r^2 = 0.32$, $F = 18.6$, $P = 0.0001$; Fig. 2a). Furthermore, the correlations between $V_{c,max}$ and A_N
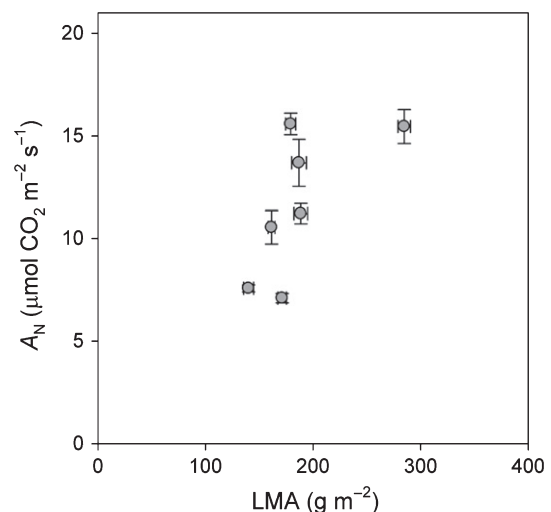

Fig. 1 Relationship between leaf mass area (LMA) and net photosynthesis (A_N) for the seven studied *Quercus* species. Data are mean ± SE.

Table 2 Photosynthetic characteristics for the seven studied *Quercus* species

Species	A_N (μmol CO_2 m^{-2} s^{-1})	g_s (mol CO_2 m^{-2} s^{-1})	iWUE (μmol mol^{-1})	g_m (mol CO_2 m^{-2} s^{-1})	V_{c,max_Cc} (μmol m^{-2} s^{-1})	J_{max_Cc} (μmol m^{-2} s^{-1})
Q. chrysolepis	13.7 ± 0.8^{de}	0.180 ± 0.020^a	56.1 ± 4.3^a	0.074 ± 0.005^{cde}	191 ± 9^a	240 ± 18^{ab}
Q. agrifolia	7.6 ± 0.2^{ab}	0.135 ± 0.017^a	38.6 ± 6.0^a	0.029 ± 0.002^a	169 ± 16^a	202 ± 12^a
Q. wislizeni	10.6 ± 1.1^{bc}	0.162 ± 0.035^a	43.1 ± 10.5^a	0.048 ± 0.009^{abc}	168 ± 9^a	206 ± 17^a
Q. coccifera	11.2 ± 0.5^{cd}	0.157 ± 0.012^a	47.1 ± 6.6^a	0.057 ± 0.006^{bcd}	188 ± 14^a	253 ± 25^{ab}
Q. ilex subsp. *ilex*	7.12 ± 0.2^a	0.095 ± 0.007^a	47.8 ± 2.9^a	0.033 ± 0.001^{ab}	195 ± 21^a	207 ± 13^a
Q. ilex subsp. rotundifolia	15.5 ± 0.8^e	0.167 ± 0.023^a	61.1 ± 5.5^a	0.080 ± 0.008^{de}	311 ± 12^b	301 ± 7^b
Q. suber	15.6 ± 0.5^e	0.170 ± 0.009^a	58.0 ± 3.4^a	0.093 ± 0.006^e	167 ± 9^a	224 ± 6^a

A_N, net photosynthesis; g_s, stomatal conductance; iWUE, intrinsic water use efficiency; g_m, mesophyll conductance to CO_2; $V_{c,max}$ and J_{max}, maximum velocity of carboxylation and maximum capacity for electron transport, respectively. Data are mean $\pm$ SE. Different letters indicate significant differences among species (Tukey's test, $P < 0.05$).
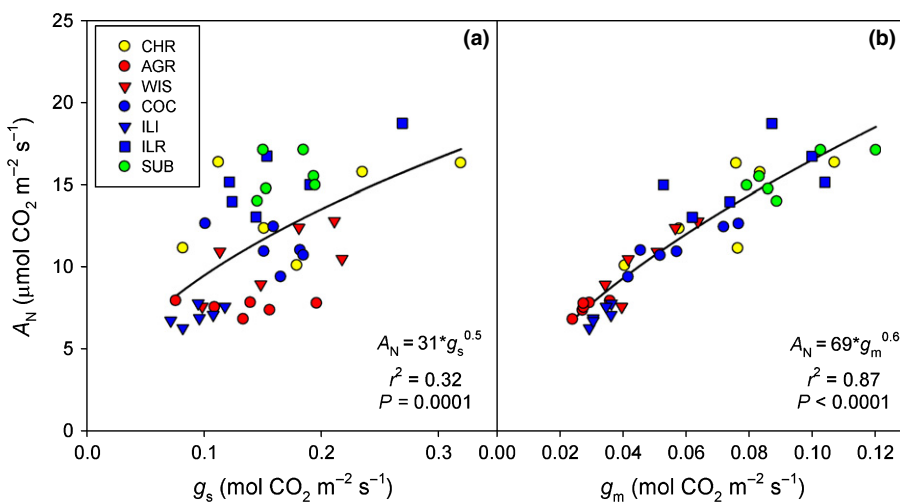

Fig. 2 Relationships between (a) stomatal conductance (g_s) and net photosynthesis (A_N) and between (b) mesophyll conductance (g_m) and net photosynthesis (A_N) for the seven studied *Quercus* species. Species abbreviations: AGR, *Q. agrifolia*; CHR, *Q. chrysolepis*; COC, *Q. coccifera*; ILI, *Q. ilex* subsp. *ilex*; ILR, *Q. ilex* subsp. rotundifolia; SUB, *Q. suber*; WIS, *Q. wislizeni*.

and between J_{max} and A_N were not statistically significant (data not shown). Analysis of the partitioning of photosynthetic limitations revealed that A_N was mainly limited by diffusional processes for all the studied species (Table 3).

Species differences in anatomical traits

The studied species displayed contrasting values of key leaf and cellular anatomical traits (Tables 4, 5). Using these traits to

Table 3 Relative stomatal (l_s), mesophyll (l_m) and biochemical (l_b) photosynthesis limitations for the seven studied *Quercus* species

Species	l_s (%)	l_m (%)	l_b (%)
Q. chrysolepis	26.6 ± 4.8^a	58.0 ± 4.9^{ab}	15.4 ± 1.3^c
Q. agrifolia	17.2 ± 2.6^a	74.9 ± 2.7^c	7.8 ± 0.2^{ab}
Q. wislizeni	20.1 ± 2.0^a	65.3 ± 2.2^{bc}	14.6 ± 1.1^c
Q. coccifera	22.8 ± 2.9^a	61.2 ± 3.4^{ab}	15.9 ± 0.8^c
Q. ilex subsp. *ilex*	24.4 ± 1.0^a	69.4 ± 0.9^{bc}	6.2 ± 0.3^a
Q. ilex subsp. rotundifolia	29.8 ± 3.4^a	60.1 ± 3.6^{ab}	10.1 ± 0.7^b
Q. suber	26.7 ± 1.6^a	48.6 ± 2.0^a	24.7 ± 0.7^d

Data are mean $\pm$ SE. Different letters indicate significant differences among species (Tukey's test, $P < 0.05$).

estimate mesophyll conductance (see the Materials and Methods section for details), a tight positive linear relationship was found between modelled and measured g_m values ($r^2 = 0.90$, $F = 43.2$, $P < 0.01$; Fig. 3), and it was clear that changes in g_m were primarily associated with specific changes in g_{liq} (Fig. 3). Measured g_m showed a tight positive linear relationship with S_c/S ($r^2 = 0.93$, $F = 84.1$, $P < 0.01$; Fig. 4a), but no correlation was detected between T_{cw} and T_{chl} and measured g_m (Fig. 4b and c, respectively). The values of T_{cw} found here are high compared to most species, and of a magnitude where their effect on $g_m/(S_c/S)$ is small (Fig. 5), pointing out that the small cell wall conductance exerts an important control on mesophyll conductance without differential effects among the studied species. The detailed analysis of individual limitations of g_m confirmed that the cell wall was the main limiting factor in all species, except *Q. ilex* subsp. rotundifolia (see Table S2). The strong influence of S_c/S in determining the specific differences in g_m also has a direct influence on net photosynthesis, as reflected in the linear relationship between S_c/S and A_N ($r^2 = 0.89$, $F = 41.9$, $P < 0.01$; Fig. 6). On the other hand, although the relationship between S_m/S and A_N for the seven studied *Quercus* species was statistically significant ($r^2 = 0.51$, $P < 0.05$; data not shown), separation of the species among two groups as a function of S_c/S_m ratio (Table 5) yielded two

Table 4 Leaf area, leaf mass area (LMA), leaf thickness, total mesophyll thickness, spongy and palisade mesophyll thickness and number of palisade layers for the seven studied *Quercus* species

Species	Leaf area (cm^2)	LMA (g m^{-2})	Leaf thickness (μm)	Mesophyll thickness (μm)	Spongy thickness (μm)	Palisade thickness (μm)	No. of palisade layers
Q. chrysolepis	3.50 ± 0.17[b]	187.6 ± 6.8[c]	281 ± 6[c]	242 ± 9[c]	124 ± 8[ab]	118 ± 4[bc]	2
Q. agrifolia	1.67 ± 0.21[a]	141.0 ± 4.7[a]	197 ± 5[a]	171 ± 5[a]	97 ± 4[a]	74 ± 4[a]	2
Q. wislizeni	5.13 ± 0.29[c]	162.2 ± 3.2[ab]	239 ± 9[b]	201 ± 8[ab]	112 ± 3[a]	90 ± 6[a]	2
Q. coccifera	1.58 ± 0.13[a]	189.3 ± 6.4[c]	315 ± 8[cd]	278 ± 7[d]	143 ± 5[b]	135 ± 3[d]	3
Q. ilex subsp. ilex	10.24 ± 0.58[d]	172.0 ± 4.0[bc]	278 ± 7[c]	240 ± 6[c]	122 ± 8[ab]	118 ± 7[bc]	2
Q. ilex subsp. rotundifolia	3.78 ± 0.33[bc]	284.9 ± 5.8[d]	348 ± 10[d]	291 ± 16[cd]	156 ± 10[b]	136 ± 6[cd]	3
Q. suber	3.69 ± 0.34[bc]	179.9 ± 4.6[bc]	228 ± 7[ab]	200 ± 8[ab]	104 ± 10[a]	96 ± 6[ab]	2

Data are mean ± SE. Different letters indicate significant differences among species (Tukey's test, $P < 0.05$).

Table 5 Fraction of the mesophyll tissue occupied by the intercellular air spaces (f_{ias}), mesophyll surface area exposed to intercellular air spaces (S_m/S), chloroplast surface area exposed to intercellular airspace (S_c/S), the ratio S_c/S_m, cell wall thickness (T_{cw}), cytoplasm thickness (T_{cyt}), chloroplast length (L_{chl}) and chloroplast thickness (T_{chl}) for the seven studied *Quercus* species

Species	f_{ias}	S_m/S (m^2 m^{-2})	S_c/S (m^2 m^{-2})	S_c/S_m	T_{cw} (μm)	T_{cyt} (μm)	L_{chl} (μm)	T_{chl} (μm)
Q. chrysolepis	0.19 ± 0.01[b]	14.2 ± 0.6[bc]	12.5 ± 0.9[b]	0.87 ± 0.03[b]	0.411 ± 0.016[cd]	0.098 ± 0.038[a]	6.28 ± 0.24[c]	3.53 ± 0.16[d]
Q. agrifolia	0.27 ± 0.02[c]	6.3 ± 0.3[a]	4.9 ± 0.4[a]	0.78 ± 0.03[b]	0.266 ± 0.013[a]	0.259 ± 0.032[b]	3.88 ± 0.23[a]	1.69 ± 0.10[ab]
Q. wislizeni	0.07 ± 0.01[a]	8.9 ± 1.8[ab]	7.8 ± 1.6[ab]	0.88 ± 0.02[b]	0.344 ± 0.015[bc]	0.045 ± 0.013[a]	4.48 ± 0.19[ab]	1.74 ± 0.08[b]
Q. coccifera	0.08 ± 0.01[a]	17.3 ± 1.8[cd]	9.9 ± 1.6[ab]	0.57 ± 0.02[a]	0.454 ± 0.026[de]	0.063 ± 0.027[a]	5.13 ± 0.23[b]	2.43 ± 0.13[c]
Q. ilex subsp. ilex	0.11 ± 0.01[a]	12.0 ± 0.9[ab]	6.5 ± 0.7[ab]	0.54 ± 0.03[a]	0.484 ± 0.014[e]	0.143 ± 0.023[ab]	5.07 ± 0.16[b]	1.80 ± 0.14[ab]
Q. ilex subsp. rotundifolia	0.07 ± 0.01[a]	21.1 ± 0.6[d]	11.5 ± 0.9[b]	0.56 ± 0.03[a]	0.362 ± 0.08[bc]	0.085 ± 0.023[a]	4.10 ± 0.21[ab]	1.17 ± 0.10[a]
Q. suber	0.10 ± 0.01[a]	16.6 ± 0.4[cd]	13.1 ± 1.0[b]	0.79 ± 0.07[b]	0.298 ± 0.012[ab]	0.101 ± 0.034[a]	4.59 ± 0.21[ab]	1.80 ± 0.08[b]

Data are mean ± SE. Different letters indicate significant differences among species (Tukey's test, $P < 0.05$).
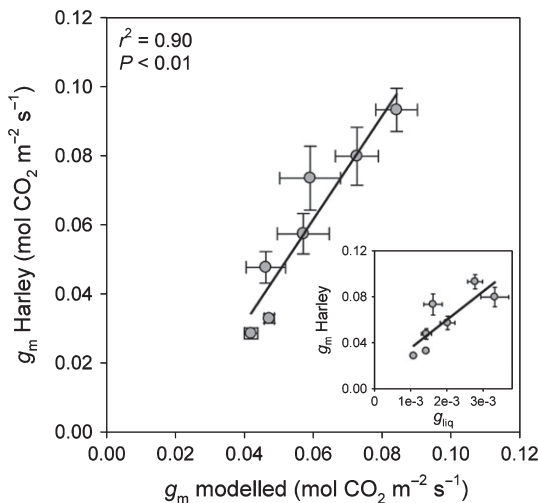

Fig. 3 Relationship between mesophyll conductance (g_m) modelled with anatomical traits and g_m measured with the Harley *et al.* (1992) method for the seven studied *Quercus* species. The inset shows the relationship between the conductance in liquid and lipid phases (g_{liq}) and g_m measured with the Harley *et al.* method ($r^2 = 0.68$, $P = 0.0228$). Data are mean ± SE.

tighter correlations (Fig. 7). The variance–covariance analysis indicated that the interaction between S_c/S_m and S_m/S was not significant, indicating that the slopes of both relationships were not statistically different at $P < 0.05$.

Discussion

This work confirms the existence of a convergence in several morphological traits among Mediterranean oaks with a diverse phylogenetic background. Such morphological leaf traits have been interpreted as adaptations to withstand summer drought (Morrow & Mooney, 1974; Poole & Miller, 1975; Baldocchi & Xu, 2007; Galmés *et al.*, 2012), given that water is the main limiting resource for plant growth in Mediterranean-type climates (Di Castri, 1981; Rhizopoulou & Mitrakos, 1990; Mediavilla & Escudero, 2003, 2004; Corcuera *et al.*, 2004). Thus, all the studied species show a reduced leaf area and thick leaves (Table 4), resulting in high LMA values when compared with other oak species from temperate climates (Corcuera *et al.*, 2002; Esteso-Martínez *et al.*, 2006). Furthermore, such convergence is common in the evergreen sclerophyllous vegetation typical for Mediterranean-type climates. Moreover, we found high values of cell wall thickness for all the studied species (Table 5; Fig. 5), similar to other evergreen tree species but higher than some deciduous trees (Tomás *et al.*, 2013). Specifically, the studied species showed T_{cw} values on average between 266 ± 13 and 484 ± 14 nm (Table 5), which were in the range reported by Hassiotou *et al.* (2010) for 18 *Banksia* species with high LMA values and by Tosens *et al.* (2012a) for 32 Australian sclerophyllous species. Besides morphological traits, the studied species shared low g_s and high iWUE values (Table 2; Fig. 2a). A reduced
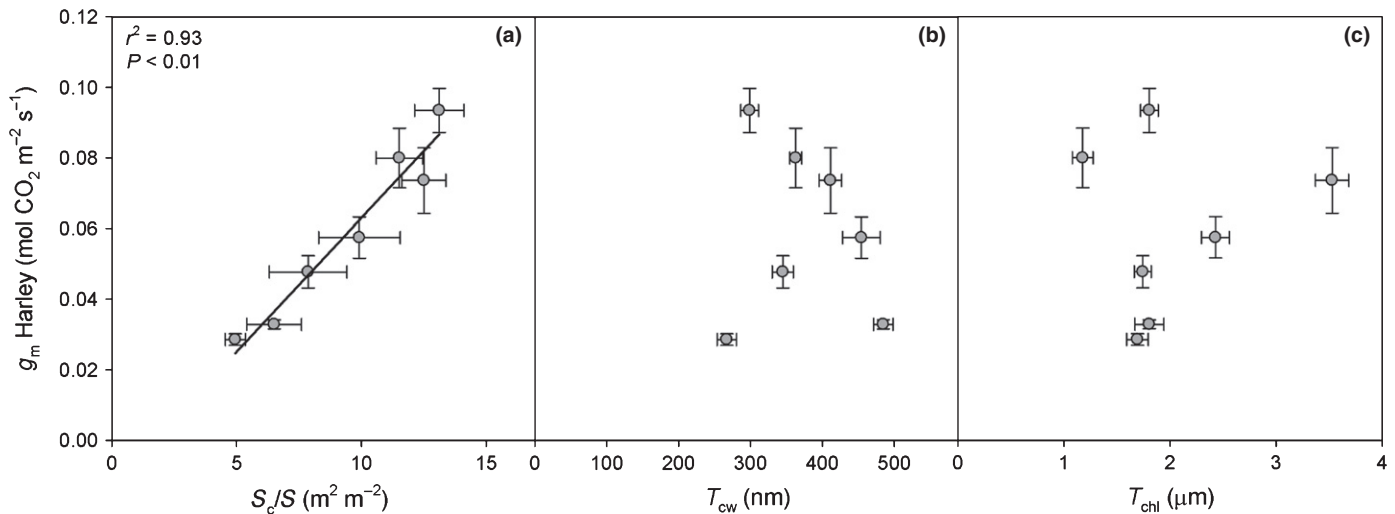
Fig. 4 Relationships between mesophyll conductance (g_m) measured with the Harley *et al.* (1992) method and (a) chloroplast surface area exposed to intercellular airspace (S_c/S), (b) cell wall thickness (T_{cw}) and (c) chloroplast thickness (T_{chl}) for the seven studied *Quercus* species. Data are mean ± SE. The relationships between g_m and T_{cw}, and between g_m and T_{chl}, were not statistically significant at $P < 0.05$.
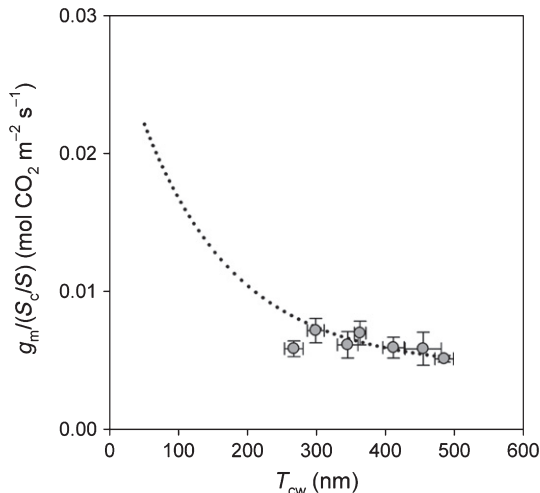

Fig. 5 Relationship between cell wall thickness (T_{cw}) and mesophyll conductance measured with the Harley *et al.* (1992) method per chloroplast surface area exposed to intercellular airspace ($g_m/(S_c/S)$) for the seven studied *Quercus* species. Data are mean ± SE. Dotted line shows the relationship found between T_{cw} and ($g_m/(S_c/S)$) by Terashima *et al.* (2011).
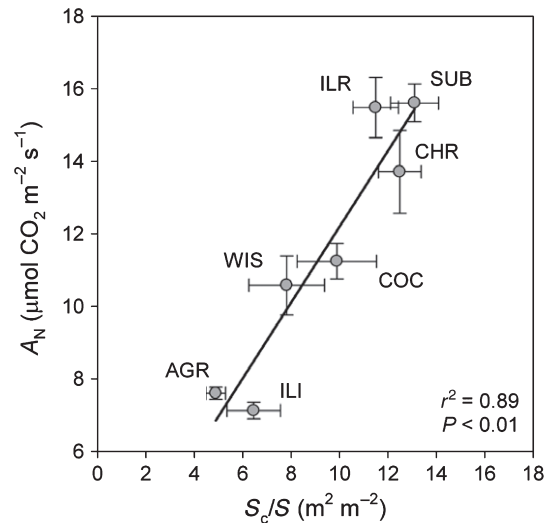

Fig. 6 Relationship between chloroplast surface area exposed to intercellular airspace (S_c/S) and net photosynthesis (A_N) for the seven studied *Quercus* species. Data are mean ± SE. Species abbreviations: AGR, *Q. agrifolia*; CHR, *Q. chrysolepis*; COC, *Q. coccifera*; ILI, *Q. ilex* subsp. *ilex*; ILR, *Q. ilex* subsp. *rotundifolia*; SUB, *Q. suber*; WIS, *Q. wislizeni*.

stomatal conductance, which is not necessarily a common feature in Mediterranean woody plants (Vilagrosa *et al.*, 2003; Peguero-Pina *et al.*, 2016b), can be interpreted in the sclerophyllous Mediterranean oaks studied here as a conservative strategy in terms of water consumption (Mediavilla & Escudero, 2003; Valladares *et al.*, 2005; Ozturk *et al.*, 2010). Moreover, the increased iWUE when compared with species from other biomes (Gulías *et al.*, 2003) has been described as an adaptive trait and a response to water scarcity in Mediterranean-type climates (Medrano *et al.*, 2009). However, despite these similarities, the present study reports the existence of differences in the photosynthetic activity among these Mediterranean evergreen oaks, which goes beyond the typical suites of morphological leaf traits reported for

evergreen sclerophyllous species. Variations in the inherent photosynthetic capacity among the studied species were not related to variations in LMA (Fig. 1) and resulted mainly from the differences in g_m (Fig. 2b), which arise from the fact that mesophyll conductance was the most limiting factor for carbon assimilation in Mediterranean oaks (Table 3), regardless of the genetic background of the studied species.

In the present study, g_m estimates modelled based on leaf anatomical properties were very similar to those estimated using the conventional method for the seven studied species (Fig. 3). In previous studies, a good correspondence was generally found between estimated g_m using both methods when largely different species are pooled in the comparison (Tosens *et al.*, 2012a, 2016;
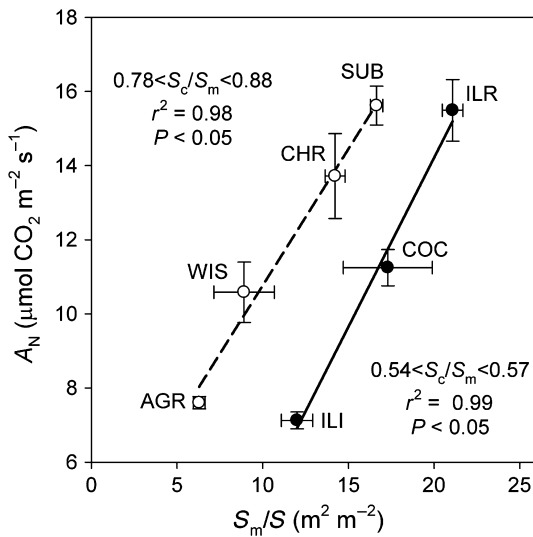
Fig. 7 Relationships between mesophyll surface area exposed to intercellular airspace (S_m/S) and net photosynthesis (A_N) for species with values for the ratio between chloroplast and mesophyll surface area exposed to intercellular airspace (S_c/S_m) between 0.78 and 0.88 (open symbols) and between 0.54 and 0.57 (closed symbols) (see Table 5). Data are mean ± SE. Species abbreviations: AGR, *Q. agrifolia*; CHR, *Q. chrysolepis*; COC, *Q. coccifera*; ILI, *Q. ilex* subsp. *ilex*; ILR, *Q. ilex* subsp. *rotundifolia*; SUB, *Q. suber*; WIS, *Q. wislizeni*.
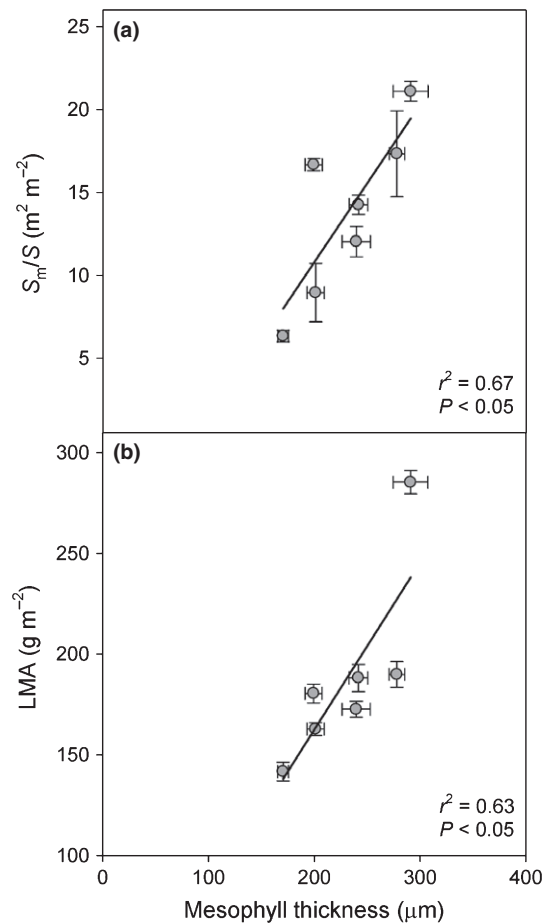

Fig. 8 Relationships between (a) mesophyll thickness and mesophyll surface area exposed to intercellular airspace (S_m/S), and between (b) mesophyll thickness and leaf mass area (LMA) for the seven studied *Quercus* species. Data are mean ± SE.

Tomás *et al.*, 2013; Carriquí *et al.*, 2015). However, such a correspondence was usually lost when comparing genotypes within a single species, especially under drought conditions (Tomás *et al.*, 2014). In this regard, Flexas *et al.* (2012) stated that g_m responds to different environmental factors (i.e. soil water availability, growth irradiance and temperature), which indicates that other additional mechanisms besides leaf anatomical traits regulate mesophyll conductance and photosynthetic activity under changing conditions. Here we have shown that the correlation between *in vivo* g_m and anatomical traits still holds under an intermediate situation when congeneric species were compared. The good correspondence between measured and simulated g_m estimates largely supports a predominant role of structural characteristics in determining photosynthetic differences among Mediterranean oaks. However, the key issue is that the contribution of different ultracellular and cellular components can vary strongly and, as our study demonstrates, the species differentiation in g_m is not necessarily determined by the most limiting component (cell walls in our study), but by components that exert a relatively minor control over total g_m. In particular, differences in g_m between the studied species can be partly attributed to the variation in leaf anatomical traits, mainly through the changes in S_c/S (Table 5; Fig. 4a) which is a key trait dominating variations in g_{liq}. In our study, species with higher photosynthetic ability have increased S_c/S and, consequently, higher g_m values with only slight changes in g_s (Fig. 2a).

From an anatomical perspective, S_c/S is determined by the combination of two independent factors, namely S_c/S_m and S_m/S. However, despite the strong lineal relationship found between S_c/S and A_N (Fig. 6), the correlations between S_c/S_m and A_N and between S_m/S and A_N were not statistically significant at $P < 0.05$

for the seven studied *Quercus* species (data not shown). Regarding S_c/S_m, in this study we have found a clear segregation in two groups among the studied species. Thus, species from the *Ilex* group showed S_c/S_m values much lower than the remaining studied species (Table 5). With respect to the second factor, S_m/S, we have found two different lineal relationships between this parameter and A_N for each group of species classified according to the two different S_c/S_m values (Fig. 7). Thus, species from the *Ilex* group required higher S_m/S values to reach net CO_2 assimilation rates similar to those showed by the other species, in order to compensate for the lower S_c/S_m ratio (Figs 7, S4), which is an anatomical factor that exerts a strong influence on g_m. This mechanism – the increase of S_m/S – must be reached at the expense of an increase in mesophyll thickness (Fig. 8).

Our results suggest that the increased S_c/S found in Mediterranean oaks can improve g_m and, consequently, net CO_2 assimilation through anatomical adaptations at the cell level. These results agree with those previously reported in several studies (Hanba *et al.*, 1999, 2002; Terashima *et al.*, 2006; Peguero-Pina *et al.*, 2016b). By contrast, Tosens *et al.* (2012a) did not find a positive correlation between S_c/S and mesophyll thickness in several Australian sclerophyllous species. Previous studies have

shown other changes in the liquid-phase component of the diffusion conductance, including modifications in cell wall thickness (Peguero-Pina *et al.*, 2012) or chloroplast thickness (Peguero-Pina *et al.*, 2016c). Again such anatomical modifications reflect the circumstance that, in most cases, g_{liq} is the strongest limitation for photosynthesis because the CO_2 diffusion coefficient in the liquid phase is four orders of magnitude smaller than that in air (Niinemets & Reichstein, 2003).

Our study was carried out in a common garden, so the specific differences in the photosynthetic performance of the Mediterranean oaks could be related to the climatic characteristics of the natural distribution ranges of each studied species. Although a prolonged summer drought period is characteristic for all these species, its severity varies somewhat across the species ranges (Table 1; Figs S2, S3). Other climatic traits also vary within and among species ranges, and such site-specific differences in the climatic characteristics could be reflected in the functional performance of the Mediterranean oaks. Indeed, species living under more continental conditions, such as *Q. chrysolepis* and *Q. ilex* subsp. *rotundifolia*, had A_N and LMA values much higher than those occurring in mild coastal areas (i.e. *Q. agrifolia* and *Q. ilex* subsp. *ilex*). In this regard, a negative linear relationship was found between the length of the vegetation period (estimated here roughly as the number of months with mean monthly temperatures above 7.5°C; Montero de Burgos & González-Rebollar, 1974) and A_N for the studied species ($r^2 = 0.67$, $P < 0.05$; Fig. S5). Therefore, the increased instantaneous photosynthetic potential found in these two species may compensate for the shortening of their vegetation period due to a combination of a negative carbon balance during winter and the drought-induced limitations of photosynthesis during summer, as previously reported by Corcuera *et al.* (2005) for *Q. ilex* subsp. *rotundifolia*. By contrast, other authors have found that Mediterranean oak species occurring at sites with milder conditions showed a positive carbon balance during winter; for example, García-Plazaola *et al.* (1999) found that *Q. ilex* subsp. *ilex* maintained photosynthetic rates during winter that were very similar to those reported in the present study in summer.

Conclusions

To the best of our knowledge, this is the first interspecific comparison of photosynthetic characteristics and underlying leaf anatomical traits among Mediterranean oaks from Europe/North Africa and North America. Despite their morphological similarity, we observed strong differences in the functional performance of individual species. We conclude that g_m is the main factor determining carbon assimilation in Mediterranean evergreen oak species. Differentiation in g_m among these species is not necessarily determined by the most limiting component (the cell wall), but by components that exert a relatively minor control over total g_m. Thus, species with higher A_N showed increased S_c/S values, which imply increased g_m values without significant changes in stomatal conductance and, therefore, water losses. The occurrence of this anatomical adaptation at the cell level allowed

evergreen oaks to reach A_N values comparable to congeneric deciduous species despite their higher LMA.

Author contributions

J.J.P-P., S.S., D.S-K. and E.G-P. planned and designed the research; S.S. and A.G-N. performed the experiments; J.J.P-P., D.S-K., J.F., J.G., U.N., M.A.S. and E.G-P. analysed the data; J.J.P-P., J.F., A.G-N., U.N. and E.G-P. wrote the manuscript.

References

Baldocchi DD, Xu L. 2007. What limits evaporation from Mediterranean oak woodlands – the supply of moisture in the soil, physiological control by plants or the demand by the atmosphere? *Advances in Water Resources* 30: 2113–2122.

Bernacchi CJ, Portis AR, Nakano H, von Caemmerer S, Long SP. 2002. Temperature response of mesophyll conductance. Implications for the determination of Rubisco enzyme kinetics and for limitations to photosynthesis in vivo. *Plant Physiology* 130: 1992–1998.

Cano FJ, Sánchez-Gómez D, Rodríguez-Calcerrada J, Warren CR, Gil L, Aranda I. 2013. Effects of drought on mesophyll conductance and photosynthetic limitations at different tree canopy layers. *Plant, Cell & Environment* 36: 1961–1980.

Carriquí M, Cabrera HM, Conesa MÀ, Coopman RE, Douthe C, Gago J, Gallé A, Galmés J, Ribas-Carbó M, Tomás M et al. 2015. Diffusional limitations explain the lower photosynthetic capacity of ferns as compared with angiosperms in a common garden study. *Plant, Cell & Environment* 38: 448–460.

Corcuera L, Camarero JJ, Gil-Pelegrín E. 2002. Functional groups in *Quercus* species derived from the analysis of pressure–volume curves. *Trees – Structure and Function* 16: 465–472.

Corcuera L, Camarero JJ, Gil-Pelegrín E. 2004. Effects of a severe drought on *Quercus ilex* radial growth and xylem anatomy. *Trees – Structure and Function* 18: 83–92.

Corcuera L, Morales F, Abadía A, Gil-Pelegrín E. 2005. Seasonal changes in photosynthesis and photoprotection in a *Quercus ilex* subsp. *ballota* woodland located in its upper altitudinal extreme in the Iberian Peninsula. *Tree Physiology* 25: 599–608.

Denk T, Grimm GW. 2009. Significance of pollen characteristics for infrageneric classification and phylogeny in *Quercus* (Fagaceae). *International Journal of Plant Science* 170: 926–940.

Di Castri F. 1981. Mediterranean-type shrublands of the world. In: Di Castri F, Goodall DW, Specht RL, eds. *Mediterranean-type shrublands*. Amsterdam, the Netherlands: Elsevier, 1–52.

Dunn OJ, Clark VA. 1987. *Applied statistics. Analysis of variance and regression.* New York, NY, USA: John Wiley & Sons Inc.

Epron D, Dreyer E, Aussenac G. 1993. A comparison of photosynthetic responses to water stress in seedlings from 3 oak species: *Quercus petraea* (Matt.) Liebl., *Q. rubra* L. and *Q. cerris* L. *Annales des Sciences Forestières* 50 (Suppl 1): 48–60.

Epron D, Dreyer E, Breda N. 1992. Photosynthesis of oak trees [*Quercus petraea* (Matt.) Liebl.] during drought under field conditions: diurnal course of net CO_2 assimilation and photochemical efficiency of photosystem II. *Plant, Cell & Environment* 15: 809–820.

Esteso-Martínez J, Valladares F, Camarero JJ, Gil-Pelegrín E. 2006. Crown architecture and leaf habit are associated with intrinsically different light-harvesting efficiencies in *Quercus* seedlings from contrasting environments. *Annals of Forest Science* 63: 511–518.

Evans JR, von Caemmerer S, Setchell BA, Hudson GS. 1994. The relationship between CO_2 transfer conductance and leaf anatomy in transgenic tobacco with a reduced content of Rubisco. *Australian Journal of Plant Physiology* 21: 475–495.

Farquhar GD, von Caemmerer S, Berry JA. 1980. A biochemical model of photosynthetic CO_2 assimilation in leaves of C_3 species. *Planta* 149: 78–90.

Flexas J, Barbour MM, Brendel O, Cabrera HM, Carriquí M, Díaz-Espejo A, Douthe C, Dreyer E, Ferrio JP, Gago J et al. 2012. Mesophyll diffusion conductance to CO_2: an unappreciated central player in photosynthesis. *Plant Science* 193–194: 70–84.

Flexas J, Díaz-Espejo A, Berry JA, Galmés J, Cifre J, Kaldenhoff R, Medrano H, Ribas-Carbó M. 2007a. Analysis of leakage in IRGA's leaf chambers of open gas exchange systems: quantification and its effects in photosynthesis parameterization. *Journal of Experimental Botany* 58: 1533–1543.

Flexas J, Díaz-Espejo A, Gago J, Gallé A, Galmés J, Gulías J, Medrano H. 2014. Photosynthetic limitations in Mediterranean plants: a review. *Environmental and Experimental Botany* 103: 12–23.

Flexas J, Ortuño MF, Ribas-Carbó M, Díaz-Espejo A, Flórez-Sarasa ID, Medrano H. 2007b. Mesophyll conductance to CO_2 in *Arabidopsis thaliana*. *New Phytologist* 175: 501–511.

Flexas J, Ribas-Carbó M, Díaz-Espejo A, Galmés J, Medrano H. 2008. Mesophyll conductance to CO_2: current knowledge and future prospects. *Plant, Cell & Environment* 31: 601–621.

Galmés J, Andralojc PJ, Kapralov MV, Flexas J, Keys J, Molins A, Parry MAJ, Conesa MÀ. 2014. Environmentally driven evolution of Rubisco and improved photosynthesis and growth within the C_3 genus *Limonium* (Plumbaginaceae). *New Phytologist* 203: 989–999.

Galmés J, Cifre J, Medrano H, Flexas J. 2005. Modulation of relative growth rate and its components by water stress in Mediterranean species with different growth forms. *Oecologia* 145: 21–31.

Galmés J, Flexas J, Medrano H, Niinemets Ü, Valladares F. 2012. Ecophysiology of photosynthesis in semi-arid environments. In: Flexas J, Loreto F, Medrano H, eds. *Terrestrial photosynthesis in a changing environment. A molecular, physiological and ecological approach*. Cambridge, UK: Cambridge University Press, 448–464.

García-Plazaola JI, Artetxe U, Becerril JM. 1999. Diurnal changes in antioxidant and carotenoid composition in the Mediterranean schlerophyll tree *Quercus ilex* L. during winter. *Plant Science* 143: 125–133.

Genty B, Briantais JM, Baker NR. 1989. The relationship between the quantum yield of photosynthetic electron transport and quenching of chlorophyll fluorescence. *Biochimica et Biophysica Acta* 990: 87–92.

González-Zurdo P, Escudero A, Babiano J, García-Ciudad A, Mediavilla S. 2016. Costs of leaf reinforcement in response to winter cold in evergreen species. *Tree Physiology* 36: 273–286.

Grassi G, Magnani F. 2005. Stomatal, mesophyll conductance and biochemical limitations to photosynthesis as affected by drought and leaf ontogeny in ash and oak trees. *Plant, Cell & Environment* 28: 834–849.

Gulías J, Flexas J, Mus M, Cifre J, Lefi E, Medrano H. 2003. Relationship between maximum leaf photosynthesis, nitrogen content and specific leaf area in Balearic endemic and non-endemic Mediterranean species. *Annals of Botany* 92: 215–222.

Hanba YT, Kogami H, Terashima I. 2002. The effect of growth irradiance on leaf anatomy and photosynthesis in *Acer* species differing in light demand. *Plant, Cell & Environment* 25: 1021–1030.

Hanba YT, Miyazawa SI, Terashima I. 1999. The influence of leaf thickness on the CO_2 transfer conductance and leaf stable carbon isotope ratio for some evergreen tree species in Japanese warm temperate forests. *Functional Ecology* 13: 632–639.

Harley PC, Loreto F, Di Marco G, Sharkey TD. 1992. Theoretical considerations when estimating the mesophyll conductance to CO_2 flux by the analysis of the response of photosynthesis to CO_2. *Plant Physiology* 98: 1429–1436.

Hassiotou F, Ludwig M, Renton M, Veneklaas EJ, Evans JR. 2009. Influence of leaf dry mass per area, CO_2 and irradiance on mesophyll conductance in sclerophylls. *Journal of Experimental Botany* 60: 2303–2314.

Hassiotou F, Renton M, Ludwig M, Evans JR, Veneklaas EJ. 2010. Photosynthesis at an extreme end of the leaf trait spectrum: how does it relate to high leaf dry mass per area and associated structural parameters? *Journal of Experimental Botany* 61: 3015–3028.

Krall JP, Edwards GE. 1992. Relationship between photosystem II activity and CO_2 fixation in leaves. *Physiologia Plantarum* 86: 80–187.

Kremer A, Abbott AG, Carlson JE, Manos PS, Plomion C, Sisco P, Staton ME, Ueno S, Vendramin GG. 2012. Genomics of Fagaceae. *Tree Genetics & Genomes* 8: 583–610.

Kummerow J. 1973. Comparative anatomy of sclerophylls of Mediterranean climatic areas. In: Di Castri F, Mooney HA, eds. *Mediterranean-type ecosystems: origin and structure*. Berlin, Germany: Springer, 213–224.

Manos PS, Doyle JJ, Nixon KC. 1999. Phylogeny, biogeography and processes of molecular differentiation in *Quercus* subgenus *Quercus* (Fagaceae). *Molecular Phylogenetics and Evolution* 12: 333–349.

Mediavilla S, Escudero A. 2003. Stomatal responses to drought at a Mediterranean site: a comparative study of co-occurring woody species differing in leaf longevity. *Tree Physiology* 23: 987–996.

Mediavilla S, Escudero A. 2004. Stomatal responses to drought of mature trees and seedlings of two co-occurring Mediterranean oaks. *Forest Ecology and Management* 187: 281–294.

Medrano H, Flexas J, Galmés J. 2009. Variability in water use efficiency at the leaf level among Mediterranean plants with different growth forms. *Plant and Soil* 317: 17–29.

Montero de Burgos J, González-Rebollar J. 1974. *Diagramas Bioclimáticos*. Madrid, Spain: ICONA.

Morrow PA, Mooney HA. 1974. Drought adaptations in two Californian evergreen sclerophylls. *Oecologia* 15: 205–222.

Niinemets Ü. 2015. Is there a species spectrum within the world-wide leaf economics spectrum? Major variations in leaf functional traits in the Mediterranean sclerophyll *Quercus ilex*. *New Phytologist* 205: 79–96.

Niinemets Ü, Keenan TF. 2014. Photosynthetic responses to stress in Mediterranean evergreens: mechanisms and models. *Environmental and Experimental Botany* 103: 24–41.

Niinemets Ü, Reichstein M. 2003. Controls on the emission of plant volatiles through stomata: a sensitivity analysis. *Journal of Geophysical Research* 108: 4211.

Niinemets Ü, Wright IJ, Evans JR. 2009. Leaf mesophyll diffusion conductance in 35 Australian sclerophylls covering a broad range of foliage structural and physiological variation. *Journal of Experimental Botany* 60: 2433–2449.

Ozturk M, Dogan Y, Sakcali MS, Doulis A, Karam F. 2010. Ecophysiological responses of some maquis (*Ceratonia siliqua* L., *Olea oleaster* Hoffm. & Link, *Pistacia lentiscus* and *Quercus coccifera* L.) plant species to drought in the east Mediterranean ecosystem. *Journal of Environmental Biology* 31: 233–245.

Peguero-Pina JJ, Flexas J, Galmés J, Niinemets Ü, Sancho-Knapik D, Barredo G, Villarroya D, Gil-Pelegrín E. 2012. Leaf anatomical properties in relation to differences in mesophyll conductance to CO_2 and photosynthesis in two related Mediterranean *Abies* species. *Plant, Cell & Environment* 35: 2121–2129.

Peguero-Pina JJ, Sancho-Knapik D, Flexas J, Galmés J, Niinemets Ü, Gil-Pelegrín E. 2016c. Light acclimation of photosynthesis in two closely related firs (*Abies pinsapo* Boiss. and *Abies alba* Mill.): the role of leaf anatomy and mesophyll conductance to CO_2. *Tree Physiology* 36: 300–310.

Peguero-Pina JJ, Sancho-Knapik D, Morales F, Flexas J, Gil-Pelegrín E. 2009. Differential photosynthetic performance and photoprotection mechanisms of three Mediterranean evergreen oaks under severe drought stress. *Functional Plant Biology* 36: 453–462.

Peguero-Pina JJ, Sisó S, Fernández-Marín B, Flexas J, Galmés J, García-Plazaola JI, Niinemets Ü, Sancho-Knapik D, Gil-Pelegrín E. 2016a. Leaf functional plasticity decreases the water consumption without further consequences for carbon uptake in *Quercus coccifera* L. under Mediterranean conditions. *Tree Physiology* 36: 356–367.

Peguero-Pina JJ, Sisó S, Sancho-Knapik D, Díaz-Espejo A, Flexas J, Galmés J, Gil-Pelegrín E. 2016b. Leaf morphological and physiological adaptations of a deciduous oak (*Quercus faginea* Lam.) to the Mediterranean climate: a

comparison with a closely related temperate species (*Quercus robur* L.). *Tree Physiology* **36**: 287–299.

Piel C. 2002. *Diffusion du CO₂ dans le mésophylle des plantes à métabolisme C₃.* PhD thesis, Paris, France: Université Paris XI Orsay.

Poole DK, Miller PC. 1975. Water relations of selected species of chaparral and coastal communities. *Ecology* **56**: 1118–1128.

Rhizopoulou S, Mitrakos K. 1990. Water relations of evergreen sclerophylls. l. Seasonal changes in the water relations of eleven species from the same environment. *Annals of Botany* **65**: 171–178.

Roupsard O, Gross P, Dreyer E. 1996. Limitation of photosynthetic activity by CO₂ availability in the chloroplasts of oak leaves from different species and during drought. *Annales des Sciences Forestières* **53**: 243–254.

Slaton MR, Smith WK. 2002. Mesophyll architecture and cell exposure to intercellular air space in alpine, desert, and forest species. *International Journal of Plant Sciences* **163**: 937–948.

Steinbrecher R, Contran N, Gugerli F, Schnitzler JP, Zimmer I, Menard T, Günthardt-Goerg MS. 2013. Inter- and intra-specific variability in isoprene production and photosynthesis of Central European oak species. *Plant Biology* **15**(Suppl. 1): 148–156.

Syvertsen JP, Lloyd J, McConchie C, Kriedemann PE, Farquhar GD. 1995. On the relationship between leaf anatomy and CO₂ diffusion through the mesophyll of hypostomatous leaves. *Plant, Cell & Environment* **18**: 149–157.

Terashima I, Hanba YT, Tazoe Y, Vyas P, Yano S. 2006. Irradiance and phenotype: comparative eco-development of sun and shade leaves in relation to photosynthetic CO₂ diffusion. *Journal of Experimental Botany* **57**: 343–354.

Terashima I, Hanba YT, Tholen D, Niinemets Ü. 2011. Leaf functional anatomy in relation to photosynthesis. *Plant Physiology* **155**: 108–116.

Thain JF. 1983. Curvature correlation factors in the measurements of cell surface areas in plant tissues. *Journal of Experimental Botany* **34**: 87–94.

Tholen D, Ethier G, Genty B, Pepin S, Zhu X. 2012. Variable mesophyll conductance revisited: theoretical background and experimental implications. *Plant, Cell & Environment* **35**: 2087–2103.

Tomás M, Flexas J, Copolovici L, Galmés J, Hallik L, Medrano H, Ribas-Carbó M, Tosens T, Vislap V, Niinemets Ü. 2013. Importance of leaf anatomy in determining mesophyll diffusion conductance to CO₂ across species: quantitative limitations and scaling up by models. *Journal of Experimental Botany* **64**: 2269–2281.

Tomás M, Medrano H, Brugnoli E, Escalona JM, Martorell S, Pou A, Ribas-Carbó M, Flexas J. 2014. Variability of mesophyll conductance in grapevine cultivars under water stress conditions in relation to leaf anatomy and water use efficiency. *Australian Journal of Grape and Wine Research* **20**: 272–280.

Tosens T, Niinemets Ü, Vislap V, Eichelmann H, Castro-Díez P. 2012b. Developmental changes in mesophyll diffusion conductance and photosynthetic capacity under different light and water availabilities in *Populus tremula*: how structure constrains function. *Plant, Cell & Environment* **35**: 839–856.

Tosens T, Niinemets Ü, Westoby M, Wright IJ. 2012a. Anatomical basis of variation in mesophyll resistance in eastern Australian sclerophylls: news of a long and winding path. *Journal of Experimental Botany* **63**: 5105–5119.

Tosens T, Nishida K, Gago J, Coopman RE, Cabrera HM, Carriquí M, Laanisto L, Morales L, Nadal M, Rojas R *et al.* 2016. The photosynthetic capacity in 35 ferns and fern allies: mesophyll CO₂ diffusion as a key trait. *New Phytologist* **209**: 1576–1590.

Traiser C, Klotz S, Uhl D, Mosbrugger V. 2005. Environmental signals from leaves – a physiognomic analysis of European vegetation. *New Phytologist* **166**: 465–484.

Turnbull MH, Whitehead D, Tissue DT, Schuster WSF, Brown KJ, Engel VC, Griffin KL. 2002. Photosynthetic characteristics in canopies of *Quercus rubra*, *Quercus prinus* and *Acer rubrum* differ in response to soil water availability. *Oecologia* **130**: 515–524.

Valentini R, Epron D, De Angelis P, Matteucci G, Dreyer E. 1995. In situ estimation of net CO₂ assimilation, photosynthetic electron flow and photorespiration in Turkey oak (*Quercus cerris* L.) leaves: diurnal cycles under different levels of water supply. *Plant, Cell & Environment* **18**: 631–640.

Valladares F, Dobarro I, Sánchez-Gómez D, Pearcy RW. 2005. Photoinhibition and drought in Mediterranean woody saplings: scaling effects and interactions in sun and shade phenotypes. *Journal of Experimental Botany* **56**: 483–494.

Vilagrosa A, Bellot J, Vallejo VR, Gil-Pelegrín E. 2003. Cavitation, stomatal conductance, and leaf dieback in seedlings of two co-occurring Mediterranean shrubs during an intense drought. *Journal of Experimental Botany* **54**: 2015–2024.

Wright IJ, Reich PB, Cornelissen JHC, Falster DS, Groom PK, Hikosaka K, Lee W, Lusk CH, Niinemets Ü, Oleksyn J *et al.* 2005. Modulation of leaf economic traits and trait relationships by climate. *Global Ecology and Biogeography* **14**: 411–421.

Wright IJ, Reich PB, Westoby M, Ackerly DD, Baruch Z, Bongers F, Cavender-Bares J, Chapin T, Cornelissen JHC, Diemer M *et al.* 2004. The world-wide leaf economics spectrum. *Nature* **428**: 821–827.

Supporting Information

Additional Supporting Information may be found online in the Supporting Information tab for this article:

Fig. S1 Geographical locations used to obtain the climatic information for the seven studied *Quercus* species throughout their distribution ranges.

Fig. S2 Ombrothermic diagrams for the distribution ranges of the seven studied *Quercus* species.

Fig. S3 Maximum daily vapour pressure deficit (VPD_{max}) for the distribution ranges of the seven studied *Quercus* species.

Fig. S4 Schematic representation of the relationships between S_m/S and A_N for species with high and low S_c/S_m values.

Fig. S5 Relationship between the length of the vegetation period and A_N for the seven studied *Quercus* species.

Table S1 Outputs of the one-way ANOVAs performed to identify the species effect on photosynthetic, morphological and anatomical traits

Table S2 Quantitative limitations of mesophyll conductance to CO₂ (g_m) in the seven studied *Quercus* species

Please note: Wiley Blackwell are not responsible for the content or functionality of any Supporting Information supplied by the authors. Any queries (other than missing material) should be directed to the *New Phytologist* Central Office.